Activation induced changes in arterial Cerebral Blood Volume (aCBV) measured using LL-EPI-STAR

M. J. Brookes[1], P. G. Morris[1], P. A. Gowland[1], S. T. Francis[1]

[1]Sir Peter Mansfield Magnetic Resonance Centre, University of Nottingham, Nottingham, United Kingdom

Introduction: The BOLD effect is caused by a combination of changes in cerebral blood flow (CBF), cerebral blood volume (CBV) and cerebral metabolic rate of oxygen extraction ($CMRO_2$), all localized to an area of neuronal activity. Original BOLD models[(1)] assumed that the change in blood volume occurred only in the venous compartment, however recent literature [(2, 3)] suggests that CBV changes also take place in the arterial compartment with changes in CBF being mediated by dilation of the muscular arterial walls. Measurement of activation-induced change in arterial CBV (aCBV) is possible using arterial spin labeling (ASL) techniques[(4)] by performing two ASL experiments across a range of TI's both with and without diffusion weighting. However, such an acquisition is time consuming, particularly if aCBV measures are required both at rest and on activation. Recently, we have shown that Look-Locher-Echo Planar Imaging (LL-EPI) [(5, 6)] can be combined with the FAIR ASL technique in order to quantify resting state aCBV[(7)]. Here, we extend our previous observations by using a STAR (Signal Targeting by Alternating Radiofrequency) modification of this technique, LL-EPI-STAR, to quantify activation-induced changes in aCBV.

Methods: The LL-EPI pulse sequence comprises a single hyperbolic secant inversion pulse followed by a series of readout pulses and EPI modules. Here, the combination of the LL-EPI sequence with STAR provides flow sensitivity. A 90 mm tagging inversion slab was centred 55 mm inferior to the imaging slice, and a 90 mm 'control' inversion slab was centred 55 mm superior to the imaging slice. The sequence was run with alternate tag and control inversions. The LL-EPI readout images repeatedly sampled labeled blood magnetization as it flowed through the imaging slice. From the difference (control – tag) images, an arterial inflow curve for each image voxel can then be obtained. Since the LL-EPI readout pulses perturb spins as they flow through the imaging slice, blood magnetization is progressively suppressed in the capillary compartment (perfusion signal). This suppression makes LL-EPI-STAR insensitive to perfusion signals whilst retaining the aCBV signal, thus allowing measurement of activation induced change in aCBV. Further, the insensitivity of LL-EPI-STAR to capillary and venous blood also ensures that measurement of activation-induced change in aCBV is not affected by oxygenation related changes in blood T_2*.

The LL-EPI-STAR sequence was implemented on a 3T MRI scanner with head gradient coil and whole head TEM RF coil. In total, 20 readout pulses were applied following each inversion pulse in order to sample adequately the arterial inflow curve. The delay between the inversion pulse and the first LL-EPI readout pulse (t_i) was 150 ms, delays between subsequent readout pulses (Δ) were 100 ms, the exception being a delay of 300 ms which was used prior to the final readout pulse in order to increase the signal to noise ratio. Following the final readout pulse, the number of EPI modules was increased from one to three to allow measurement of the standard BOLD effect from the first echo, and ΔT_2* by fitting the multi-echo set. The delay (TR) between LL-EPI-STAR sets was 3 s. MBEST EP images with an in-plane resolution of 4 x 4 mm and a slice thickness of 6 mm were acquired using a matrix size of 64 x 64, an echo time of 35 ms and flip angle of 50°. Spoiler gradients were employed between pulses in order to prevent stimulated echoes.

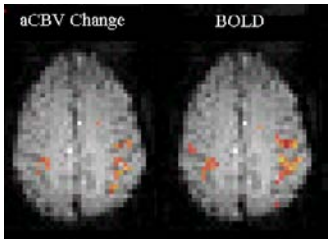

Figure 1: Areas of activation identified using aCBV signal (Left) and the BOLD response (right).

Four healthy volunteers took part in the study. The paradigm involved a blocked finger-tapping task cued visually. Initially 10 LL-EPI sets were acquired in order to allow for T_1 saturation effects. Following this, the paradigm commenced, in which each cycle comprised 30 s of bilateral finger tapping followed by 30 s of rest. This meant that a total of 20 LL-EPI sets (and hence 10 difference image sets) were acquired during each cycle, resulting in the difference image sets having an effective temporal resolution of 6 s. A total of 14 cycles were acquired in order to allow signal averaging.

Analysis: Data were motion corrected and smoothed using a 5mm FWHM Gaussian smoothing kernel. In order to identify areas of stimulus related change in aCBV, difference images 3 to 8 from each LL-EPI set were averaged in order to obtain a single aCBV weighted image every 6 s. (Images 3 to 8 were chosen as this is where the greatest change in signal was observed in the difference images (Figure 2).) Pixel timecourses from these aCBV weighted images were then smoothed temporally using a 5 s FWHM kernel, and correlated with the stimulus waveform convolved with a hrf in Medx. Z-statistical images showing stimulus correlated change in aCBV were thresholded at 2.3 and overlaid onto a single slice. Pixels of interest were identified from these z-statistical maps and used to derive regions of interest for further study. LL-EPI inflow curves were extracted from difference images for these ROI's for both rest and active periods and averaged across cycles. These inflow curves were then normalized using the M_0 of arterial blood, which was estimated from signals in the large cerebral arteries. Resulting inflow curves (Figure 2) were then fitted to a previously described model[(7)] in order to calculate aCBV at rest and on activation. Regions of significant BOLD effect were assessed based on the first echo following the final readout pulse. Areas of significant BOLD contrast were identified using a correlation analysis in Medx.

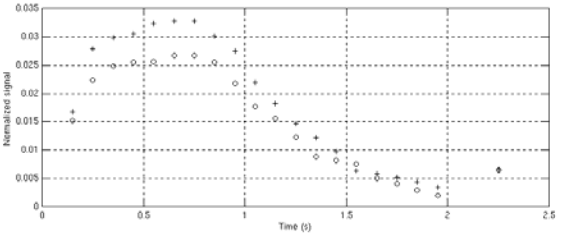

Figure 2: Normalized LL-EPI-STAR signals for activation (crosses) and rest (circles) in a representative subject.

Subject	*aCBV (rest)*	*aCBV (active)*
1	*3.5 %*	*5.6 %*
2	*1.3 %*	*1.6 %*
3	*3.7 %*	*4.9 %*
4	*6.2 %*	*7.5 %*

Table 1: Quantitative aCBV values for activation and rest, taken from regions of interest in motor cortex derived using correlation analysis.

Results: Figure 1 shows areas of significant aCBV change and BOLD contrast for a single representative subject. Active areas in the aCBV map are more focal, and overlay areas of significant BOLD contrast. Figure 2 shows the normalized LL-EPI-STAR inflow curves taken from a region of interest during both rest (circles) and activation (crosses). Across subjects *(n=4)*, the inflow signal during activation was found to peak earlier than that during rest, and to be higher in amplitude. Table 1 shows the results of the quantitative analysis of the LL-EPI-STAR signals. Results show that in all subjects, an increase in aCBV was observed during activation when compared to the resting state (p=0.02, paired t-test).

Discussion: We have shown that the LL-EPI-STAR sequence can be employed in order to measure quantitatively activation-induced changes in arterial cerebral blood volume. The sequence can also be used to derive spatial patterns of significant change in both aCBV, and BOLD contrast. Arterial CBV values reported in Table 1 show variability across subjects, we expect this effect to arise due to the difference in the regions of interest identified by the correlation analysis. If these regions contain large cerebral arteries then aCBV values will, in general, be high when compared to regions containing only small arterioles. Figure 2 shows that the LL-EPI-STAR sequence allows characterization of the inflow curves with high temporal resolution for both activation and rest, this represents a major advantage of LL-EPI over other more traditional methods [(4)]. Further, the implemented LL-EPI-STAR sequence is not sensitive to CBF changes, venous volume changes, or changes in blood T_2*.

Acknowledgements: This Work is supported by a Programme Grant from the Medical Research Council (MRC).

References: 1) Buxton *et al*., MRM, 39, 855-864, 1998. 2) Lee *et al*., MRM, 45, 791-800, 2001. 3) Duong *et al*. MRM, 43, 393-402, (2003). 4) Hoad *et al*, Proc. 12th ISMRM (2004). 5) Look & Locher, Rev. Sci. Inst, 41, 250-1 (1970). 6) Gowland and Mansfield, MRM 30 351-354 (1993) 7) Brookes *et al*, Proc. 13th ISMRM (2005).